Proceedings of ESDA2006
8th Biennial ASME Conference on Engineering Systems Design and Analysis
July 4-7, 2006, Torino, Italy

ESDA2006-95539

NUMERICAL INVESTIGATION ON LOAD TRANSFER EFFECTS IN BOGIES OF URBAN RAIL VEHICLES

Roberto Corradi
Politecnico di Milano
Via G. La Masa,34
20156 Milano, Italy
roberto.corradi@polimi.it

Alan Facchinetti
Politecnico di Milano
Via G. La Masa,34
20156 Milano, Italy
alan.facchinetti@polimi.it

Giovanni Sempio
Politecnico di Milano
Via G. La Masa,34
20156 Milano, Italy
giovanni.sempio@tiscali.it

ABSTRACT

Urban rail vehicles can present many types of architecture, definitely different from those of traditional rail vehicles. When dealing with long articulated tramcars, complex coupling effects between the vertical and lateral dynamics may arise. Making reference to a modern tramcar, the coupling phenomena are investigated in detail by means of numerical simulation, considering the dynamic behaviour during the negotiation of curves with or without superelevation.

INTRODUCTION

Modern urban rail vehicles are characterized by structural configurations and design solutions (e.g. articulated bogie frames, independently rotating wheels) which can significantly differ from those of traditional rail vehicles. Moreover they present a modular architecture that allows to arrange different configurations. Generally two different bodies can be identified in the vehicle assembly: a type-A module, that is composed of a carbody and a bogie, and a type-B module, which is a single carbody, suspended between two type-A modules. In this way vehicles can conform administrations' requests, setting a specific length and a defined capacity. Figure 1 shows some types of modern low-floor tramcars, actually in use in two European cities. Both vehicles are composed of 7 modules.

Long tramcars are particularly subjected to considerable load transfers within the same axle or between the two axles of a bogie, that may lead to dynamic problems. In particular, the decrease of the vertical load on a wheel may lead to reduced braking/driving efficiency and, in extreme cases, to safety issues. Furthermore urban rail vehicles are characterised by frequent acceleration/deceleration transients that accentuate these problems.

On the basis of all these considerations, careful analysis of vehicle dynamics by means of proper numerical simulations is needed, from the very beginning of the design process.

Figure 1: Two typical modern tramcars with 7-bodies architecture.

Making reference to a 7-carbodies tramcar, numerical investigations on load transfer phenomena in typical operating conditions are carried out. All the time-domain simulations presented in this paper are performed by means of a mathematical model [1,7], that has been extensively validated [5], specifically designed for reproducing the structural configurations and wheel-rail contact conditions typical of urban rail vehicles.

VEHICLE NUMERICAL MODEL

A numerical model specific for simulating urban rail vehicle dynamics has been developed at Politecnico di Milano [1,7]. This fully non-linear model allows to analyse the non-stationary behaviour of a tramcar, running in tangent and curved track, eventually with variable speed. To this end, combined longitudinal, lateral and vertical vehicle motion is considered. Carbodies are schematized as rigid bodies, while bogie frames and wheelsets flexibility is considered because of its strong influence on vehicle dynamics. The most common configurations of modern tramcars can be reproduced by the combination of two types of basic modules:

- module A, which is made up of one carbody and one bogie;
- module B, which is a single carbody, suspended between two type A modules.

The different modules are linked one to each other by means of kinematic constraints and/or elastic and viscous elements, which reproduce the actual connections between the carbodies.

As an example, Figure 2 shows the model of the 7-carbodies tramcar that is considered in this paper.

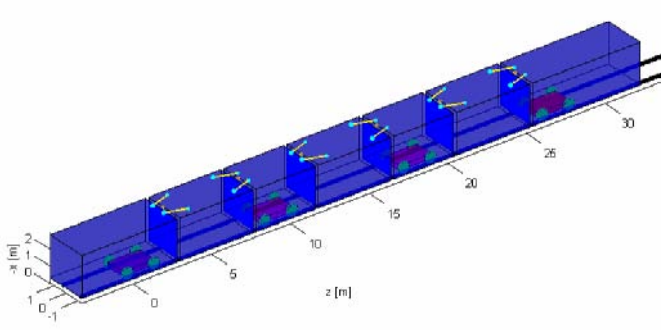

Figure 2: numerical model of a 7-bodies articulated tramcar (4 type A modules and 3 type B modules).

The equations of motion of each A module are written with respect to an auxiliary moving frame of reference (*track frame of reference*), travelling with variable speed along the ideal track centreline and following the carbody centre of gravity. The relative motion of the module components with respect to this moving reference is considered through modal superposition approach: the equations of motion are written in terms of the generalised coordinates corresponding to the rigid/flexible natural modes of each module component, considered free from any mutual/global constraint. Then the single components of each A-module are coupled by means of elastic and damping elements, reproducing the primary and secondary suspensions.

Following this approach, each i[th] A-module is described using the following coordinates:

$$\underline{x}_i^T = \left[s_i \quad \underline{q}_{ci}^T \quad \underline{q}_{bi}^T \quad \underline{q}_{fwi}^T \quad \underline{q}_{rwi}^T \right] \qquad (1)$$

where s_i is the curvilinear abscissa corresponding to the position of the carbody's centre of gravity along the ideal track centreline, and $\underline{q}_{ci}$, $\underline{q}_{bi}$, $\underline{q}_{fwi}$ and $\underline{q}_{rwi}$ are the modal coordinates relevant to carbody, bogie, front wheelset and rear wheelset. In this way, the total motion of each A-module is obtained by superimposing the small displacements of the single components on the gross motion of the overall module.

The equations of motion of each type-B module are written by considering the gross motion of a *carbody coordinate system* with respect to the *global coordinate system*. The origin of the carbody coordinate system is rigidly attached to the centre of gravity and its axes are the carbody principal axes.

Each j[th] B-module is then described using the following coordinates:

$$\underline{x}_j^T = \left[x_{Gj} \quad y_{Gj} \quad z_{Gj} \quad \sigma_j \quad \beta_j \quad \rho_j \right] \qquad (2)$$

where x_{Gj}, y_{Gj} and z_{Gj} identify the position of the carbody's centre of gravity with respect to the global coordinate system and σ_j, β_j and ρ_j are the Cardano angles which define the orientation of the carbody coordinate system with respect to the global frame of reference.

The equations of motion of the complete vehicle are obtained applying Lagrange's equations and can be written in the following matrix form:

$$[M(\underline{x})]\ddot{\underline{x}} + [C]\dot{\underline{x}} + [K]\underline{x} = \underline{Q}(\underline{x}, \dot{\underline{x}}, t)$$

$$\underline{Q} = \underline{Q}_m + \underline{Q}_c + \underline{Q}_{nl} + \underline{Q}_{cf} \qquad (3)$$

where:

- $\underline{x}$ is the vector containing the whole model independent variables and is composed by the coordinates $\underline{x}_i$ and $\underline{x}_j$ of each module (equations (1), (2)):
- $[M]$, $[C]$ and $[K]$ are the mass, damping and stiffness matrices of the whole tramcar model;
- vector $\underline{Q}$ contains the generalised forces associated with the non-linear terms related to vehicle's inertia $\underline{Q}_m$, the connections between carbodies $\underline{Q}_c$, the effects of non linear elastic elements (e.g. bumpstops) $\underline{Q}_{nl}$ and the non-linear wheel-rail contact forces $\underline{Q}_{cf}$, which also account for track irregularity excitation.

With reference to the $\underline{Q}_{cf}$ term, the model adopted for the calculation of the forces acting at wheel-rail interface is suitable for reproducing the contact phenomena which are typical of tramcar operation [4]. In particular, it is designed to account for the out of plane contacts which occur as a consequence of the not negligible wheel-rail yaw angle in low radius curves, as well as for the presence of multiple contact points on the tread and the flange, also in case of presence of a grooved rail (Figure 3).

The normal forces are evaluated through a multi-Hertzian model [12], while Shen-Edrick-Elkins formulation is used to calculate the forces acting in the tangential plane [14].

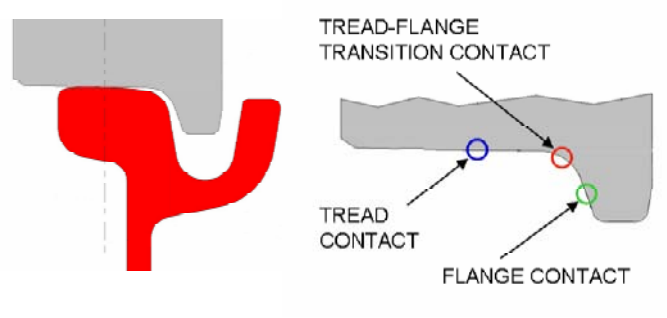

Figure 3: numerical model of wheel-rail coupling, with multiple contact points on the wheel-rail interface.

CURVE WITHOUT SUPERELEVATION

The first case analysed deals with the simulation (through the numerical model described in the previous paragraph) of the load transfer effect on a curve without superelevation. A modern low-floor articulated tramcar, equipped with non-conventional bogies with independently rotating wheels is considered. This tramcar is composed by a sequence of 7 modules (Figure 2): starting from the leading one, type-A and type-B modules alternate.

The results reported hereafter refer to the vehicle running at 20 km/h on a left curve of radius R=61m (0.5m/s^2 lateral acceleration), followed by a short straight track section. Since in this paper attention is focused on the steady-state load transfers in curve, the numerical simulations are performed considering an ideal, perfectly smooth track.

Figure 4 shows the calculated time-histories of the vertical loads acting on the four wheels of the first bogie. Looking at this figure, the typical load transfer between the two wheels of the same axle can be observed: vertical load is transferred from the inner wheels to the outer ones.

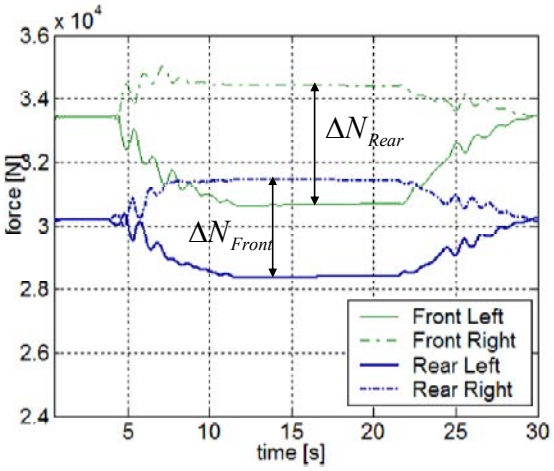

Figure 4: Vertical forces on the wheels of the two axles (first module). Left curve without superelevation, radius=61m, cant deficiency=0.5m/s^2.

In general, the load transfer between left and right wheels is caused by the centrifugal force in curve and/or other type of lateral forces, such as those due to wind action. As a consequence of the forces exchanged with the carbody, the bogie is subjected to a roll angle which is the main responsible for the load transfers. On the basis of this consideration one would expect the load transfers on the front and rear axles to be equal. But this is not the case of Figure 4.

Obviously there must be some additional effect: indeed the primary suspension on the two wheelsets is subjected to a deformation also in the lateral direction. When a bogie yaw arises, the different shear deformation of the front and rear suspension influences the load transfer on the two axles.

To better understand the cause of this effect, the equilibrium on the single axle is considered. Figure 5 shows the forces acting on a wheelset, in the vertical plane. In this picture the following forces are represented:

- Q_{ps} vertical load transmitted by the primary suspension;
- T_{ps} roll torque transmitted by the primary suspension;
- Y_{ps} lateral shear force transmitted by the primary suspension;
- Q_{LW} left wheel vertical load;
- Q_{RW} right wheel vertical load;
- F_{RIPAGE} acting at track level.

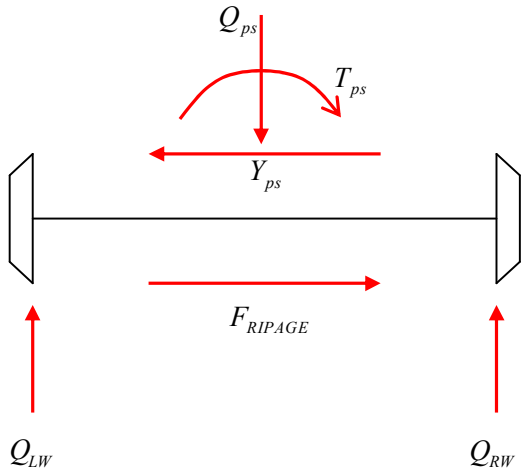

Figure 5: Forces acting on the axle of a bogie in the vertical plane.

The forces Q_{ps} on the front and rear primary suspension are generally different and are mainly dependent on the vehicle mass distribution. Anyway, Q_{ps} does not influence the load transfer. Moreover, assuming rigid bogie frame, the steady-state roll torque T_{ps} on the front and rear primary suspension in full curve is equal, and therefore also this contribution can not be the responsible for the effect under study.

A detailed analysis on the role of the lateral force Y_{ps} is presented hereafter. Considering a single A-module in steady-state curve negotiation, the primary suspension is forced to react to the global carbody lateral force resulting from the

centrifugal force and the forces exchanged at the connections with the adjacent carbodies. Consequently, for each axle, the lateral deformation of the primary suspension generates the shear force Y_{ps}, which is balanced by the ripage force F_{RIPAGE}, acting at track level. Observing Figure 5, it is evident that these two forces generate an additional roll torque, which is responsible for the differential load transfer between the two wheels of the same axle. In fact, if the lateral loads on the two axles (ripage forces) are different, also the load transfers must be different for the equilibrium to be satisfied. In other words, the load transfers on the axles would be equally distributed only if the two wheelset ripage forces were identical.

Ripage forces on the two axles of a single bogie can be different because of many reasons. Figure 6 shows the two components of the global carbody lateral force, acting on the leading module of the tramcar presented in figure 2: inertial force and connections force. These forces are balanced only by the ripage forces on the two axles.

The ripage force distribution must satisfy the equilibrium not only in the lateral direction, but also in the yaw direction. Considering that the bogie is equipped with independently rotating wheels, there is no yaw torque on the wheelsets, due to longitudinal forces acting at wheel/rail interface. As a consequence, the ripage force unbalance is simply associated with the dissymmetries related to the position of the module centre of gravity, or to the forces exchanged at the linkages of the carbodies.

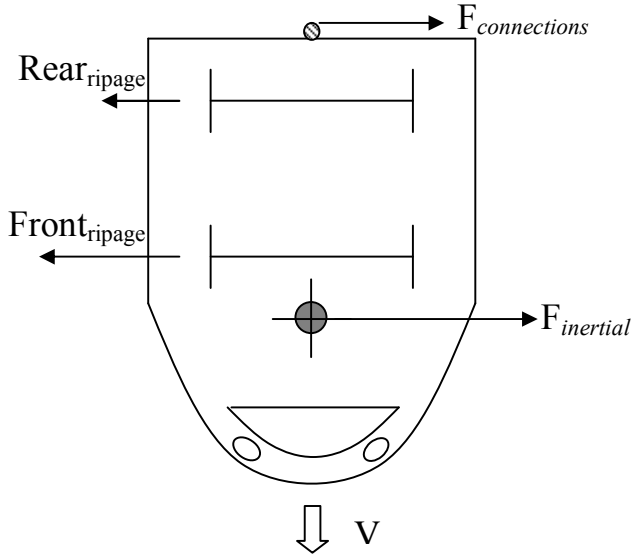

Figure 6: Forces acting on the first module of the tramcar, in the horizontal plane.

Considering the typical architecture of modern tramcars, such as those reported in figure 1, it is obvious that dissymmetry effects are more pronounced on the modules at vehicle extremities, while central bogies are generally characterised by a substantially homogeneous distribution of the ripage forces. As a consequence, load transfers are usually more uniformly distributed on the central bogies than on the external ones.

CURVE WITH SUPERELEVATION

In the previous paragraph a curve without superelevation has been considered. Now attention is focused on the opposite case, of a curve with superelevation. The additional effects associated with the presence of cant are pointed out, together with the influence of vehicle architecture.

First of all, it is important to notice that the phenomenon related to the ripage forces previously analysed is always present, also for curves with superelevation. In order to seek for possible supplementary outcomes specific for this case, the same left curve (R=61m) has been simulated, but introducing 50mm of superelevation. The tramcar speed is now increased at 26 km/h, so as to maintain the same cant deficiency (0.5m/s^2).

Figure 7 shows the calculated time-histories of the vertical loads acting on the four wheels of the first bogie. By making a comparison between the results of the curve without superelevation (Figure 4) and of the curve with superelevation (Figure 7), significant differences arise, both in steady-state and in transient condition.

Looking at the steady-state response in the curve with superelevation (Figure 7, 9-17s), the main difference with respect to figure 4 is represented by the mean values of the vertical forces on the two wheels of the front/rear axles (see the horizontal dash-dot lines in Figure 7). By comparing the values of the wheel load before entering the curve and in case of vehicle in full curve, the mean wheel load itself increases from 33kN to 38kN on the front axle, from 30kN to 31.5kN on the rear one. In other words, the axle load raises on both axles, but more markedly on the front one. As will be shown in figure 10, the 4th and last bogie has the same kind of behavior.

This means that: a) load is transferred from the inner bogies to external ones; b) a pitch rotation of the first module's carbody seems to be induced by the presence of the superelevation, which is responsible for the non-uniform growth of the loads on the two axles.

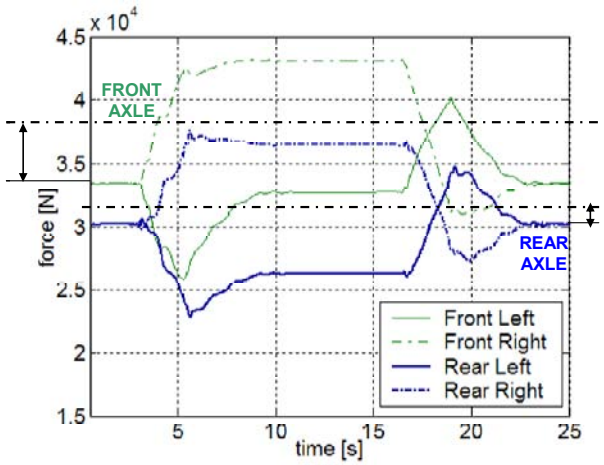

Figure 7: Vertical forces on the wheels of the two axles (first module). Left curve with superelevation, radius=61m, cant deficiency=0.5m/s^2..

To better understand the influence of the superelevation, it is essential to make reference to a sketch of the first three modules in the tramcar assembly (Figure 8). In this figure the three carbodies are represented with large relative yaw angles,

always present during the negotiation of a curve. In fact typical tramways are characterized by very narrow curves, and this causes big relative yaw angles between different modules.

If the first module is rolled of a quantity ρ_1 as a consequence of the superelevation, this rotation is transmitted to the following modules, through the connections between the carbodies. Thus the roll angle on the first module has a double effect: a vertical displacement and a pitch rotation of the third module. In fact the roll angle ρ_1 of the first module can be resolved on the third module into two components: the roll angle ρ_3 and the pitch angle β_3. Similar considerations can be made starting from the third module and moving to the first one.

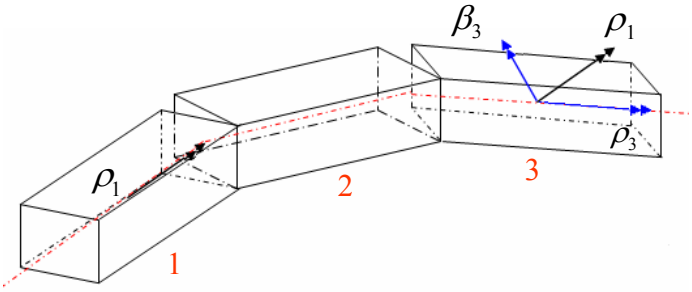

Figure 8: Coupling effect due to the relative yaw angles between carbodies and to the presence of superelevation as a consequence of the connections between different modules.

These effects related to the coupling of carbody roll and pitch motion, have a strong influence on load transfer mechanisms and are particularly important in case of:

- sharp curve negotiation and consequent large relative yaw angles between the carbodies;
- curve superelevation leading to carbody roll;
- long tramcars (in this case, both the previous phenomena are amplified).

In particular, the carbody roll angles are related to the classical load transfer between left and right wheels, while the pitch angles are responsible for the load transfer between the front and rear axles of the same bogie.

Making reference to the 7-modules tramcar schematically shown in figure 9, the combination of track curvature and cant is responsible for the load transfer from the inner bogies to external ones. Moreover, the opposite pitch rotations of the first and last module justify the non-uniform, specular distribution of the axle loads on the external bogies (Figure 9): as a result, the most loaded axles are the first and the last ones. The vertical arrows in Figure 9 indicate load increase when directed upwards, load decrease when directed downwards.

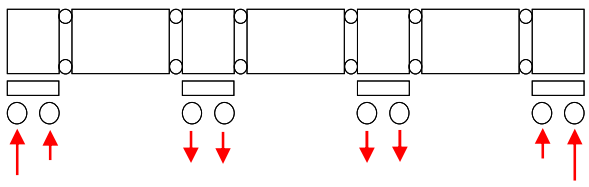

Figure 9: Load transfer on the different axles of the tramcar.

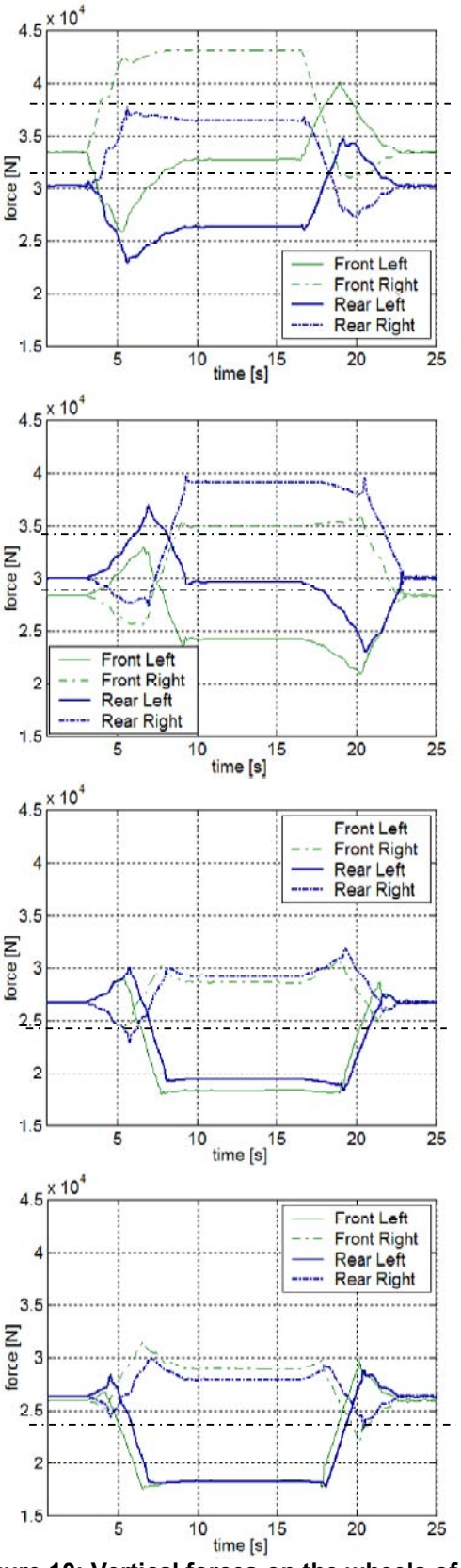

Figure 10: Vertical forces on the wheels of the tramcar. Left curve with superelevation, radius=61m, cant deficiency=0.5m/s^2.

Figure 10 shows the results of the numerical simulations, in terms of vertical wheel/rail contact forces time-histories, for all the bogies the 7-modules tramcar reported in Figure 9. These results show that on the two inner modules there are no significant differences in terms of mean vertical wheel load on the front and rear axles: a fairly uniform bogie unloading can be observed. On the contrary, considering the two bogies at vehicle extremities, vertical load increases on both axles, but not uniformly. The front axle of the first module is loaded more than the rear axle; the opposite situation occurs on the last module.

All the numerical results presented up to now refer to the vehicle architecture schematically indicated in Figure 9. It is obvious that the typology of the connections between the carbodies strongly influences the load transfer phenomena described above. It is also obvious that the configuration of Figure 9 (the linkages between the carbodies block both relative pitch and roll) is the worst one, in terms of amplification of the load transfer effects.

In order to investigate the effect of vehicle architecture, the numerical simulations have been repeated, by changing the connections between the carbodies (Figure 11), so as to increase the tramcar degrees of freedom. In more detail, the upper linkages between the 2nd and 3rd modules and between the 5th and 6th modules have been released. These loose connections can not transmit roll and pitch torques any more. Consequently, apart from carbody relative yaw, the tramcar behaves as if it was composed of three separate blocks: the first composed by the first two modules, the second by the three central ones, the third by the last two modules. Each of these three blocks can be considered as a rigid body, in terms of pitch and roll rotation.

By reducing the carbody constraints, the load transfer effects illustrated in figure 10 are strongly reduced as it can be observed by the comparison with figure 12, which refers to the new vehicle configuration.

Figure 12 shows that load transfers between the axles of extremity modules disappear, as a consequence of upper linkages modification. Moreover, in this case, load transfer between left and right side are more relevant than other load transfer effects along the vehicle.

It is worth remarking that, in both vehicle configurations, the load transfers between the different axles are symmetrical with respect to the vehicle mid-length (Figures 9 and 11), as a consequence of the symmetric architecture of the considered tramcar.

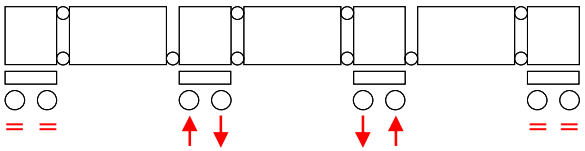

Figure 11: Load transfer on the different axles of the tramcar (released upper linkages).

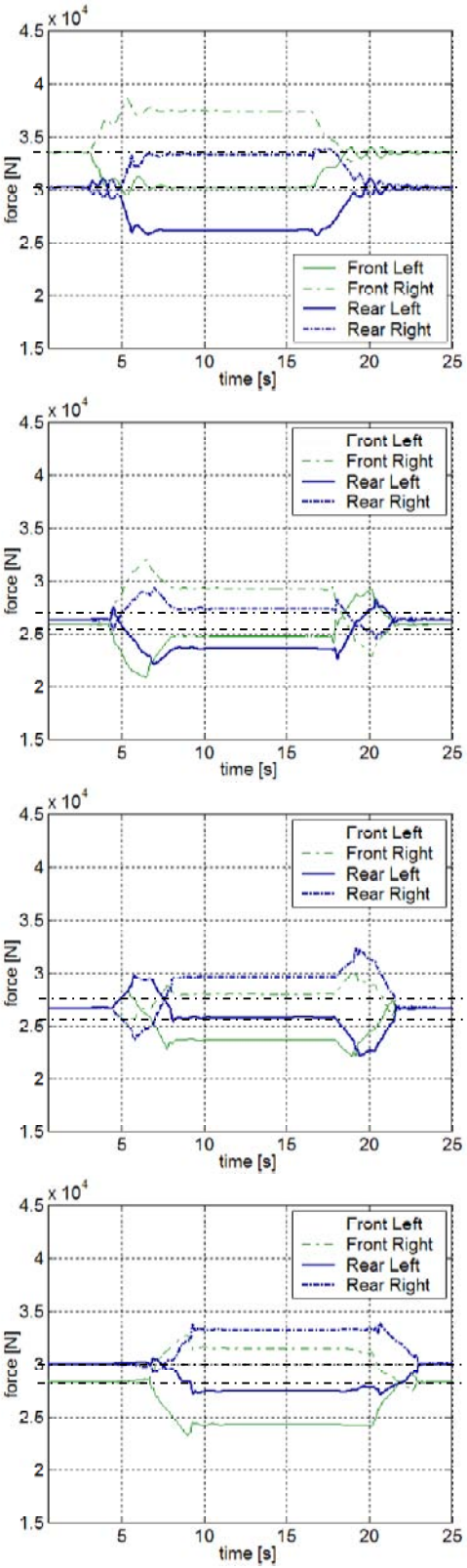

Figure 12: Vertical forces on the wheels of the tramcar(released upper linkages). Left curve with superelevation, radius=61m, cant deficiency=0.5m/s^2.

CONCLUSION

In this paper load transfers on the axles articulated tramcars have been investigated, considering the coupling effects between the vertical and lateral dynamics, particularly important in presence of curve superelevation.

Load transfers lead to wheels unloading and possibly , as a consequence, to difficulties in traction/braking transmission and to a decrease of running safety. For these reasons load transfer effects should be considered at tramcar design stage in order to reduce their impact on vehicle dynamic behaviour.

Numerical models can be adopted to perform parametric analyses on the influence of different vehicle features, such as carbodies lengths, bogies pitch, connections between adjacent modules and secondary suspensions characteristics. By making numerical simulations an optimal configuration can be obtained and load transfers can be minimized.

REFERENCES

1. BELFORTE P, CHELI F, CORRADI R, FACCHINETTI A, **A Software for the Numerical Simulation of Tramcar Vehicle Dynamics**, *New Developments in Heavy Vehicle Simulation*, special issue of the *International Journal of Heavy Vehicle Systems*, 2003
2. BRUNI S, COLLINA A, DIANA G, VANOLO P, **Lateral Dynamics of a Railway Vehicle in Tangent Track and Curve: Tests and Simulation**, *XVI IAVSD Symposium*, Pretoria, South Africa,1999
3. CHELI F, BERETTA S, BELFORTE P, BUCCA G, DESIMONE H, **Structural Integrity Analysis of a Tram-Car Line: Force Wand Material Damage**, *6th International Conference on Contact Mechanics and Wear of Rail/Wheel Systems (CM2003),* Gothenburg, Sweden, 2003
4. CHELI F, CORRADI R, DIANA G, FACCHINETTI A, **Wheel-Rail Contact phenomena and Derailment Conditions in Light Urban Vehicles**, *6th International Conference on Contact Mechanics and Wear of Rail/Wheel Systems (CM2003),* Gothenburg, Sweden, 2003
5. CHELI F, CORRADI R, DIANA G, FACCHINETTI A, **Experimental Validation of a Numerical Model for the Simulation of Tramcar Vehicle Dynamics**, *2005 IASME International Design Engineering Conferences and Computers and Information in Engineering Conference (IDETC/CIE 2005),* Long Beach, California, USA, 2005
6. CHELI F., CORRADI R., DIANA G., MANIGRASSO R., MAPELLI F., **Tangent track and curve control strategies for tramcar bogies with independently driven wheels**, *ERRI Interactive Conference, Mechatronics for trains: essential technology for the future?*, Paris, France, 2002
7. CHELI F, CORRADI R, FACCHINETTI A, **A Numerical Model to Analyse the Dynamic Behaviour of Modern Tramcars**, *VSDIA 2002*, Budapest, Hungary, 2002
8. CHELI F., CORRADI R., MAPELLI F., MAURI M., **Motion control of a bogie with independently motorised wheels**, Proc. of the *10th Int. Power Electronics and Motion Control Conference*, Cavtat & Dubrovnik, Croatia, 2002
9. ELKINS J A, CARTER A, **Safety Assessment of Rail Vehicles**, *Vehicle System Dynamics*, Vol.22, N. 3-4, 1993
10. KALKER J J, **Three-Dimensional Elastic Bodies in Rolling Contact**, Kluwer Academic Publisher, 1990
11. KIK W, MOELLE D, BORGO C, FERRAROTTI G, **Adams/Rail – Medyna statement of the method**, *The Manchester Benchmarks for Rail Vehicle Simulation, Supplement to Vehicle System Dynamics,* Vol. 31, 1999
12. PASCAL J P, **The Available Methods to Calculate the Wheel/Rail Forces in Non-Hertzian Contact Patches and Rail Damaging**, *Vehicle System Dynamics*, Vol. 22, 1993
13. SHABANA A A, **Dynamics of Multibody Systems**, Cambridge University Press, 1998
14. SHEN Z Y, HEDRICK J K, ELKINS J A, **A Comparison of Alternative Creep-Force Models for Rail Vehicle Dynamic Analysis**, *VIII IAVSD Symposium*, 1983